Supporting Information - Accuracy of XH-stretching Intensities with the Deng-Fan Potential

Emil Vogt[†], Daniel S. Sage[‡], and Henrik G. Kjaergaard[*†]

[†]Department of Chemistry, University of Copenhagen, Universitetsparken 5, DK-2100, Copenhagen Ø, Denmark
[‡]Department of Mathematics, Louisiana State University, Baton Rouge, LA 70806, USA

[*]hgk@chem.ku.dk

1 Deng-Fan Wave Functions and Energy Levels

The Schrödinger equation for a diatomic DF oscillator is [1]

$$\frac{-\hbar^2}{2\mu}\frac{d^2\Psi(r)}{dr^2} + D\frac{[1-\exp(-a(r-r_e))]^2}{[1-\exp(-ar)]^2}\Psi(r) = E\Psi(r), \tag{1.1}$$

and the exact analytical bound state energy levels are [2]

$$E_v = D - \frac{D}{4\kappa}\left(v + d - \frac{B\kappa}{v+d}\right)^2, \tag{1.2}$$

where $B = \exp(2ar_e)-1$, $\kappa = \frac{2\mu D}{a^2\hbar^2}$, $d = \frac{1}{2}(1+(1+4\kappa b^2)^{1/2})$ and $b = \exp(ar_e)-1$ are all constants. Eq. 1.2 is obtained by first introducing the dimensionless variable $x = ar$. Eq. 1.1 can then be written as

$$\left(-\frac{d^2}{dx^2} + \kappa\left(1 - \frac{b}{\exp(x)-1}\right)^2\right)\psi(x) = \frac{2\mu E}{a^2\hbar^2}\psi(x) \equiv \epsilon\psi(x), \tag{1.3}$$

where $\Psi(r) = \sqrt{a}\psi(x)$. Eq. 1.3 can be solved analytically by introducing another dimensionless variable $y = (\exp(x)-1)^{-1}$ and the function $F(y)$ [1, 2].

$$\psi(x) = \Phi(y) = \frac{y^\alpha}{(1+y)^\beta}F(y). \tag{1.4}$$

This transforms eq. 1.3 to the following form

$$y(y+1)\frac{d^2F(y)}{dy^2} + [2(\alpha-\beta+1)y + (2\alpha+1)]\frac{dF(y)}{dy} + [(\alpha-\beta)^2 + \alpha - \beta + C]F(y) = 0. \tag{1.5}$$

Provided that α, β and C are chosen to satisfy the following relations:

$$\alpha = \sqrt{\kappa - \epsilon} = \sqrt{\frac{2\mu(D-E)}{a^2\hbar^2}} \tag{1.6}$$

$$\beta = \sqrt{\alpha^2 + \kappa b(b+2)} = \sqrt{\kappa(b+1)^2 - \epsilon} = \sqrt{\frac{2\mu}{a^2\hbar^2}[D(b+1)^2 - E]} \tag{1.7}$$

$$C = -\kappa b^2 = -\frac{2\mu}{a^2\hbar^2}b^2 D \tag{1.8}$$

eq. 1.5 can be satisfied if $F(y)$ is the hypergeometric function ${}_2F_1(l, e; 2\alpha+1; -y)$, where $l = \alpha - \beta + d$, $e = \alpha - \beta + 1 - d$ and $d = \frac{1}{2}\left(1 + \sqrt{1-4C}\right) = \frac{1}{2}\left(1 + \sqrt{1+4\kappa b^2}\right)$. For bound states $l = -v$, with v being a nonnegative integer. From eq. 1.7 and the definition of l, it is evident that both α and β are dependent on v, and combining the two equations yields

$$\alpha_v = \frac{1}{2}\left(\frac{\kappa b(b+2)}{v+l} - v - d\right) \quad \& \quad \beta_v = \frac{1}{2}\left(\frac{\kappa b(b+2)}{v+l} + v + d\right) = \alpha_v + v + d. \tag{1.9}$$

By rearranging eq. 1.6 to $\epsilon = \kappa - \alpha^2$, one obtains the exact analytical bound state energy levels (eq. 1.2). The corresponding orthonormal eigenfunction are

$$\Psi_v(r) = |v\rangle = N_v y^{\alpha_v}(1+y)^{-\beta_v}{}_2F_1(-v, 1-v-2d; 2\alpha_v+1; -y), \tag{1.10}$$

with the normalization constant, N_v, being [2]

$$N_v = \left(\frac{a(\alpha_v+v+d)\Gamma(2\alpha_v+v+1)\Gamma(2\alpha_v+v+2d)}{v!(v+d)\Gamma(v+2d)\Gamma(2\alpha_v)\Gamma(2\alpha_v+1)}\right)^{1/2}. \tag{1.11}$$

The gamma function of x+2d, appearing in eq. 1.11, is a very large number and consequently troublesome to evaluate in some programs. It can be useful to gather the gamma function of $2\alpha_v + v + 2d$, in the numerator, and the two gamma functions involving $v + 2d$ and $2\alpha_v$, in the

denominator, as one divided by the beta function of $v+2d$,$2\alpha_v$. The beta function is defined in eq. 2.9. The hypergeometric function defined as [3]

$$ {}_2F_1(-v, 1-v-2d; 2\alpha_v+1; -y) = \sum_{n=0}^{\infty} \frac{(-v)_n (1-v-2d)_n}{(1+2\alpha_v)_n n!} (-y)^n, \tag{1.12} $$

where the Pochhammer symbol $(z)_n$ is equivalent to the rising factorial ($(z)_n = \Gamma(z+n)/\Gamma(z)$). Eq. 1.12 reduces to a v'th order polynomial in y, since $(-v)_n$ is zero for integers where $n > v$ [4]. Parameters of the Deng-Fan potential can be obtained from experimental transition frequencies using [5]

$$ \frac{\tilde{\nu}_{v\leftarrow 0}}{v} = \frac{D(v+2d)}{4\kappa h c} \left(\left(\frac{B\kappa}{d(v+d)} \right)^2 - 1 \right). \tag{1.13} $$

This equation is obtained from subtracting eq. 1.2 for $v=0$ from eq. 1.2 for a general v, and then dividing with v.

2 Derivation of Displacement Matrix Elements

Matrix elements in the displacement coordinate can be calculated from matrix elements of integral powers of the coordinate, by using the binomial theorem

$$ (r-r_e)^j = r^j - \binom{j}{1} r_e r^{j-1} + \binom{j}{2} r_e^2 r^{j-2} - \binom{j}{3} r_e^3 r^{j-3} + ... + (-1)^j r_e^j. \tag{2.1} $$

The first step is to calculate the following matrix elements

$$ \langle u | \exp(\lambda a r) | v \rangle = \left\langle u \left| \left(\frac{y+1}{y} \right)^{\lambda} \right| v \right\rangle. \tag{2.2} $$

The equality follows from

$$ \left\langle u \left| \left(\frac{y+1}{y} \right)^{\lambda} \right| v \right\rangle = \left\langle u \left| \left(\frac{\frac{y}{y} + \frac{1}{y}}{\frac{y}{y}} \right)^{\lambda} \right| v \right\rangle = \left\langle u \left| \left(\frac{\exp(ar) - 1 + 1}{1} \right)^{\lambda} \right| v \right\rangle. \tag{2.3} $$

This integral can be calculated analytically by expressing the integrand as positive powers of y and negative powers of $(y+1)$. Given that [3]

$$ \int_0^{\infty} dy \frac{y^{\alpha}}{(y+1)^{\beta}} = \frac{\Gamma(\alpha+1)\Gamma(\beta-\alpha-1)}{\Gamma(\beta)}. \tag{2.4} $$

To go from eq. 2.2 to eq. 2.4 requires changing the coordinate of integration from r to y.

$$ \frac{dy}{dr} = \frac{d}{dr} \left(\exp(ar) - 1 \right)^{-1} = -a \exp(ar) \left(\exp(ar) - 1 \right)^{-2} = -a \left(\frac{y+1}{y} \right) y^2 = -a (y+1) y. \tag{2.5} $$

We now solve eq. 2.2 for the Deng-Fan wave functions (eq. 1.10). Since the wave functions are real, we omit taking the complex conjugate of the wave function in the bra.

$$\begin{aligned}
\left\langle u \left| \left(\frac{y+1}{y}\right)^{\lambda} \right| v \right\rangle &= \int_{r=0}^{r=\infty} dr \Psi_u(r) \left(\frac{y+1}{y}\right)^{\lambda} \Psi_v(r) \\
&= \int_{y=\infty}^{y=0} \frac{dy}{-a\,(y+1)\,y} \Psi_u(r) \left(\frac{y+1}{y}\right)^{\lambda} \Psi_v(r) \\
&= \frac{1}{a} \int_{y=0}^{y=\infty} \frac{dy}{(y+1)\,y} \Psi_u(r) \left(\frac{y+1}{y}\right)^{\lambda} \Psi_v(r) \\
&= \frac{1}{a} \int_{y=0}^{y=\infty} dy \Psi_u(r) \frac{y^{-1-\lambda}}{(y+1)^{1-\lambda}} \Psi_v(r) \qquad (2.6) \\
&= \frac{1}{a} \int_{y=0}^{y=\infty} dy \Bigg(N_u y^{\alpha_u} (1+y)^{-\beta_u} \sum_{m=0}^{u} \frac{(-u)_m (1-u-2d)_m}{(1+2\alpha_u)_m m!} (-y)^m \frac{y^{-1-\lambda}}{(y+1)^{1-\lambda}} \\
&\quad \times N_v y^{\alpha_v} (1+y)^{-\beta_v} \sum_{n=0}^{v} \frac{(-v)_n (1-v-2d)_n}{(1+2\alpha_v)_n n!} (-y)^n \Bigg) \\
&= \frac{N_v N_u}{a} \sum_{n=0}^{v} \sum_{m=0}^{u} (-1)^{n+m} \frac{(-u)_m (1-u-2d)_m (-v)_n (1-v-2d)_n}{(1+2\alpha_u)_m m! (1+2\alpha_v)_n n!} \\
&\quad \times \int_{y=0}^{y=\infty} dy \frac{y^{-1-\lambda+\alpha_u+\alpha_v+n+m}}{(y+1)^{1-\lambda+\alpha_v+\alpha_u+v+u+2d}}.
\end{aligned}$$

In the first step the coordinate and boundaries of integration are changed. In the second step the boundaries of integration are swapped, thereby removing the minus sign in the denominator. The third step is to reformulate the integrand in accordance with eq. 2.4. Now, the wave functions $\Psi_v(r)$ and $\Psi_u(r)$ are expressed in terms of eq. 1.10. Finally, we insert the definition of β from eq. 1.9 and write $(-y)^n(-y)^m$ as $(-1)^{n+m}y^{n+m}$. The term $(-1)^{n+m}$ was presumably forgotten in the paper by Rong and Sage from 2009 [4]. It is now possible to use eq. 2.4 to obtain;

$$\begin{aligned}
\left\langle u \left| \left(\frac{y+1}{y}\right)^{\lambda} \right| v \right\rangle =& \frac{N_u N_v}{a} \sum_{n=0}^{u} \sum_{m=0}^{v} (-1)^{n+m} \frac{(-u)_n (-v)_m (1-u-2d)_n (1-v-2d)_m}{(1+2\alpha_u)_n (1+2\alpha_v)_m \Gamma(n+1)\Gamma(m+1)} \qquad (2.7) \\
&\times \frac{\Gamma(\alpha_u+\alpha_v+n+m-\lambda)\Gamma(2d+u+v-n-m+1)}{\Gamma(\alpha_u+\alpha_v+2d+u+v+1-\lambda)},
\end{aligned}$$

here $m!$ and $n!$ is written as $\Gamma(m+1)$ and $\Gamma(n+1)$, respectively. Evaluating eq. 2.7 for $\lambda = 0$ and abbreviating the summand as $C_0(u,n,v,m)$ yields the analytical overlap matrix elements

$$\langle u|v\rangle = \frac{N_u N_v}{a} \sum_{n=0}^{u} \sum_{m=0}^{v} C_0(u,n,v,m). \qquad (2.8)$$

In terms of numerical precision and computational cost, it can be useful to express the last term in eq. 2.7 as the beta function [3]

$$B(x,y) \equiv \frac{\Gamma(x)\Gamma(y)}{\Gamma(x+y)} = \int_0^{\infty} dt \frac{t^{x-1}}{(1+t)^{x+y}}. \qquad (2.9)$$

Matrix elements of integral powers of the coordinate can be found as derivatives of eq. 2.7 with respect to λ

$$\frac{d^l}{d\lambda^l} \left\langle u \left| \left(\frac{y+1}{y}\right)^{\lambda} \right| v \right\rangle \Bigg|_{\lambda=0} = \frac{d^l}{d\lambda^l} \langle u| \exp(\lambda a r) |v\rangle \Big|_{\lambda=0} = a^l \langle v|r^l|v\rangle. \qquad (2.10)$$

The matrix elements can now be written as

$$\langle v|r^l|v\rangle = \frac{1}{a^l} \frac{d^l}{d\lambda^l} \left\langle u \left| \left(\frac{y+1}{y}\right)^{\lambda} \right| v \right\rangle \Bigg|_{\lambda=0}. \qquad (2.11)$$

In eq. 2.7, only two gamma functions contain the parameter λ and consequently the derivative of these gamma functions needs to be specified. Derivatives of the gamma function can be related to the digamma function, $\psi(x)$, and polygamma functions, $\psi^{(l)}(x)$

$$\psi(x) = \frac{\frac{d}{dx}\Gamma(x)}{\Gamma(x)} \quad \& \quad \psi^{(l)}(x) = \frac{d^l}{dx^l}\psi(x). \tag{2.12}$$

As a consequence of eq. 2.12, taking the first derivative of eq. 2.7 will yield the original term, abbreviated as $C_0(u, n, v, m)$ multiplied by the difference of the two digamma functions. We show this by abbreviating $\alpha_u + \alpha_v + n + m$ as A and $\alpha_u + \alpha_v + 2d + u + v + 1$ as B.

$$\begin{aligned}
\frac{d}{d\lambda}\left(\frac{\Gamma(A-\lambda)}{\Gamma(B-\lambda)}\right) &= \frac{1}{\Gamma(B-\lambda)}\left(\frac{d}{d\lambda}\Gamma(A-\lambda)\right) + \Gamma(A-\lambda)\frac{d}{d\lambda}\frac{1}{\Gamma(B-\lambda)}. \\
&= -\left(\frac{\psi(A-\lambda)\Gamma(A-\lambda)}{\Gamma(B-\lambda)} - \frac{\Gamma(A-\lambda)\psi(B-\lambda)\Gamma(B-\lambda)}{\Gamma(B-\lambda)^2}\right) \\
&= \frac{\Gamma(A-\lambda)}{\Gamma(B-\lambda)}\left(\psi(B-\lambda) - \psi(A-\lambda)\right)
\end{aligned} \tag{2.13}$$

where the minus in front comes from taking the derivative of $-\lambda$ with respect to λ. The difference of these two digamma functions, evaluated at $\lambda = 0$, is denoted by $C_1(u, n, v, m)$

$$C_1(u, n, v, m) = \big[\psi(\alpha_u + \alpha_v + 2d + u + v + 1) - \psi(\alpha_u + \alpha_v + n + m)\big]. \tag{2.14}$$

The last equations needed to obtain analytical oscillator strengths of the Deng-Fan potential are displayed in full in the article.

3 Transition Frequencies

In Table 1, we present calculated and experimental transition frequencies. The single point potential energy calculations are at the CCSD(T)/aug-cc-pVTZ (aug-cc-pV(T+d)Z for Cl) level of theory. In the first row, the molecule of interest is presented with a subscript expressing which type of potential energy surface is used to calculate the transition frequencies in that row. The subscript Morse indicates that the Morse potential is used, DF, that the Deng-Fan potential is used, Num, that a numeric potential is used, and lastly Expt. indicates that the transition frequencies are experimentally determined.

Table 1: Experimental and calculated XH-stretching transition frequencies in cm^{-1}.

Molecule	$\Delta v = 1$	$\Delta v = 2$	$\Delta v = 3$	$\Delta v = 4$	$\Delta v = 5$
HF_{Morse}	3953.8	7737.3	11350.4	14793.3	18065.9
HF_{DF}	3953.8	7737.3	11355.7	14813.9	18116.6
HF_{Num}	3952.7	7735.5	11351.3	14803.1	18093.4
$HF_{Expt.}$ [a]	3961.4	7750.8	11372.8	14831.7	18131.0
HCl_{Morse}	2888.7	5670.8	8346.3	10915.2	13377.4
HCl_{DF}	2888.7	5670.8	8348.1	10922.8	13396.8
HCl_{Num}	2890.0	5674.1	8352.8	10924.9	13396.4
$HCl_{Expt.}$ [b]	2885.9	5668.0	8346.9	10923.1	13396.5
OH_{Morse}	3555.9	6948.6	10178.1	13244.4	16147.4
OH_{DF}	3555.9	6948.6	10182.9	13263.3	16194.3
OH_{Num}	3556.8	6951.5	10184.3	13254.8	16162.9
$OH_{Expt.}$ [c]	3569.6	6973.7	10214.1	13291.8	16207.1
$HCOOH_{Morse}$	3584.5	7007.0	10267.6	13366.2	16302.9
$HCOOH_{DF}$	3584.5	7007.0	10272.3	13384.9	16349.4
$HCOOH_{Num}$	3587.9	7017.4	10290.8	13409.9	16377.2
$HCOOH_{Expt.}$ [d]	3568.9	6968.3	10200	13284.1	16160
CH_3OH_{Morse}	3674.4	7180.0	10516.7	13684.4	16683.4
CH_3OH_{DF}	3674.4	7180.0	10521.7	13704.1	16731.8
CH_3OH_{Num}	3676.9	7185.6	10526.3	13698.4	16701.4
$CH_3OH_{Expt.}$ [e]	3683.9	7196.1	10525.6	13704.6	16705.9 [f]
$HNO_{3,Morse}$	3564.4	6971.6	10221.8	13314.8	16250.7
$HNO_{3,DF}$	3564.4	6971.6	10226.3	13333.1	16296.3
$HNO_{3,Num}$	3568.3	6981.2	10241.0	13349.6	16309.1
$HNO_{3,Expt.}$ [g]	3551	6940	10173	13245	16160

[a] Experimental frequencies from Ref. [6] and HITRAN [7]
[b] Experimental frequencies from Refs. [8, 9] and HITRAN [7]
[c] Experimental frequencies from HITRAN [7]
[d] Experimental frequencies from refs. [10, 11, 12, 13]
[e] Experimental frequencies from ref. [14]
[f] This band couples to the combination band of one quantum in the methyl asymmetric stretch and four quanta in the OH-stretch. The value given is calculated from a deperturbation analysis, using CD_3OH as the reference of the unperturbed system. The observed spectral splitting is $\sim$50 cm^{-1} with the pure OH-band being blue-shifted by $\sim$25 cm^{-1} [15].
[g] Experimental frequencies from refs. [16, 17, 18]

4 Coefficients of Dipole Moment Functions

In Table 2, we present coefficients for the dipole moment functions obtained by a linear least-squares fitting to points in the range $r - r_e = [-0.4$ Å ; 0.9 Å,] in steps of 0.05 Å around the equilibrium geometry. The dipole moment vector at each point is calculated using a finite field approach, with an applied field strength of ±0.0001 a.u. [19] at the CCSD(T)/aug-cc-pVTZ (aug-cc-pV(T+d)Z for Cl) level of theory.

Table 2: Coefficients of polynomial dipole moment functions.

Molecule	μ_1[D/Å]	μ_2[D/Å^2]	μ_3[D/Å^3]	μ_4[D/Å^4]	μ_5[D/Å^5]	μ_6[D/Å^6]
HF	1.5252	-0.1024	-1.0521	-0.3788	-0.7836	0.7737
HCl	0.9157	-0.0208	-0.6903	-0.2723	0.0917	0.2455
OH	0.4720	-0.6846	-0.7350	-0.0927	-0.1338	0.4106
HCOOH-y	1.0333	-0.6314	-0.7532	-0.2476	0.2028	0.1201
HCOOH-z	0.4019	0.2732	-0.4283	-0.1627	-0.1644	0.1610
CH_3OH-y	0.5660	-0.8177	-1.2368	-0.0738	0.7423	0.0150
CH_3OH-z	0.4197	-0.8446	-0.5208	-0.0802	0.5297	-0.0487
HNO_3-y	-0.2000	0.6011	-0.1272	-0.0453	-0.1305	0.1351
HNO_3-z	-1.3660	0.1885	0.7958	0.4988	0.0454	0.1035

5 Parameters of Analytical Potentials

In Table 3, we present parameters obtained for Morse potentials and Deng-Fan potentials with the pure *ab initio* approach. Equilibrium bond lengths (r_e) are found from a CCSD(T)/aug-cc-pVTZ/FC optimization (aug-cc-pV(T+d)Z for Cl).

Table 3: Morse and Deng-Fan parameters obtained with the pure *ab initio* approach.

Molecule	r_e[Å]	D_{DF}[cm^{-1}]	a_{DF}[Å^{-1}]	D_M[cm^{-1}]	a_M[Å^{-1}]	$\tilde{\nu}_e$[cm^{-1}]	$\tilde{\nu}_e X_e$[cm^{-1}]
HF	0.9210	61988	1.4620	48760	2.2251	4124.2	87.21
HCl	1.2764	49942	1.3153	42023	1.7616	2996.0	53.40
OH	0.9736	52725	1.4578	42301	2.1440	3718.7	81.73
HCOOH	0.9701	54504	1.4297	43359	2.1340	3747.4	80.97
CH_3OH	0.9611	54097	1.4972	43611	2.1831	3844.8	84.74
HNO_3	0.9723	55098	1.4023	43549	2.1166	3725.1	79.66

Table 4: Parameters obtained for Morse potentials and Deng-Fan potentials from the experimental transition frequencies presented in Table 1. All experimental transition frequencies are utilized, except for $\Delta v = 5$ for methanol. The calculated r_e values are used for the Deng-Fan potential.

Molecule	D_{DF}[cm^{-1}]	a_{DF}[Å^{-1}]	D_M[cm^{-1}]	a_M[Å^{-1}]	$\tilde{\nu}_e$[cm^{-1}]	$\tilde{\nu}_e X_e$[cm^{-1}]
HF	63153	1.4434	50832	2.1810	4127.5	83.79
HCl	50439	1.3026	43253	1.7323	2989.0	51.64
OH	50346	1.5371	42477	2.1478	3733.2	82.03
HCOOH	48625	1.5851	41693	2.1695	3736.0	83.69
CH_3OH	51828	1.5659	43087	2.2028	3856.1	86.28
HNO_3	51832	1.4796	43182	2.1168	3709.8	79.67

In Table 5, we present experimentally determined bond dissociation energies. The zero-point vibrational energy has not been added to the values presented in Table 5.

Table 5: Experimental dissociation energies in cm^{-1}

	HF[a]	HCl[b]	OH[c]	HCOOH[d]	CH_3OH[a]	HNO_3[e]
D_0	47653±4	36077±11	35591±24	39172±1049	36583±245	36371±351

[a] Taken from ref. [20]
[b] Taken from ref. [21]
[c] Taken from ref. [22]
[d] Taken from ref. [23]
[e] Taken from ref. [24]

6 Oscillator Strengths

In Table 6, we present all calculated oscillator strengths with both the pure *ab initio* and the semi-empirical approach. For the semi-empirical approach, all experimental transition frequencies are utilized, except for $\Delta v = 5$ for methanol as this transition is strongly coupled with the combination band of one quantum in the methyl asymmetric stretch and four quanta in the OH-stretch [15]. The experimental transition frequencies can be found in Table 1 and the fitted parameters in Table 4. The same dipole moment function is used for the pure *ab initio* and the semi-empirical approach, and the coefficients can be found in Table 2.

Table 6: Calculated oscillator strengths with the pure *ab initio* and semi-empirical approach.

Calculated Oscillator Strengths - Pure *Ab Initio*					
Molecule	$\Delta v = 1$	$\Delta v = 2$	$\Delta v = 3$	$\Delta v = 4$	$\Delta v = 5$
HF_{Morse}	1.83×10^{-5}	5.07×10^{-7}	1.01×10^{-8}	2.79×10^{-10}	6.58×10^{-12}
HCl_{Morse}	6.44×10^{-6}	1.50×10^{-7}	9.08×10^{-10}	1.02×10^{-12}	2.45×10^{-12}
OH_{Morse}	1.46×10^{-6}	2.32×10^{-7}	8.54×10^{-9}	3.92×10^{-10}	2.27×10^{-11}
$HCOOH_{Morse}$	9.33×10^{-6}	4.97×10^{-7}	1.83×10^{-8}	1.06×10^{-9}	9.57×10^{-11}
CH_3OH_{Morse}	3.17×10^{-6}	5.90×10^{-7}	2.34×10^{-8}	1.12×10^{-9}	8.90×10^{-11}
$HNO_{3,Morse}$	1.50×10^{-5}	5.55×10^{-7}	2.02×10^{-8}	1.38×10^{-9}	1.40×10^{-10}
HF_{DF}	1.82×10^{-5}	5.92×10^{-7}	1.89×10^{-8}	1.13×10^{-9}	9.74×10^{-11}
HCl_{DF}	6.41×10^{-6}	1.70×10^{-7}	2.04×10^{-9}	2.16×10^{-11}	9.88×10^{-14}
OH_{DF}	1.43×10^{-6}	2.45×10^{-7}	1.19×10^{-8}	8.55×10^{-10}	8.81×10^{-11}
$HCOOH_{DF}$	9.23×10^{-6}	5.50×10^{-7}	2.67×10^{-8}	2.17×10^{-9}	2.68×10^{-10}
CH_3OH_{DF}	3.09×10^{-6}	6.20×10^{-7}	3.17×10^{-8}	2.25×10^{-9}	2.55×10^{-10}
$HNO_{3,DF}$	1.48×10^{-5}	6.27×10^{-7}	3.01×10^{-8}	2.73×10^{-9}	3.59×10^{-10}
HF_{Num}	1.82×10^{-5}	5.65×10^{-7}	1.62×10^{-8}	8.50×10^{-10}	6.08×10^{-11}
HCl_{Num}	6.42×10^{-6}	1.62×10^{-7}	1.50×10^{-9}	7.80×10^{-12}	2.01×10^{-13}
OH_{Num}	1.44×10^{-6}	2.41×10^{-7}	1.08×10^{-8}	6.99×10^{-10}	6.57×10^{-11}
$HCOOH_{Num}$	9.27×10^{-6}	5.33×10^{-7}	2.39×10^{-8}	1.80×10^{-9}	2.07×10^{-10}
CH_3OH_{Num}	3.12×10^{-6}	6.09×10^{-7}	2.86×10^{-8}	1.81×10^{-9}	1.88×10^{-10}
$HNO_{3,Num}$	1.49×10^{-5}	6.05×10^{-7}	2.71×10^{-8}	2.31×10^{-9}	2.89×10^{-10}
Calculated Oscillator Strengths - Semi-Empirical					
HF_{Morse}	1.83×10^{-5}	4.88×10^{-7}	8.89×10^{-9}	2.19×10^{-10}	3.89×10^{-12}
HCl_{Morse}	6.44×10^{-6}	1.45×10^{-7}	7.64×10^{-10}	2.48×10^{-12}	2.72×10^{-12}
OH_{Morse}	1.46×10^{-6}	2.31×10^{-7}	8.53×10^{-9}	3.93×10^{-10}	2.28×10^{-11}
$HCOOH_{Morse}$	9.31×10^{-6}	5.09×10^{-7}	1.97×10^{-8}	1.18×10^{-9}	1.11×10^{-10}
CH_3OH_{Morse}	3.16×10^{-6}	5.92×10^{-7}	2.41×10^{-8}	1.18×10^{-9}	9.52×10^{-11}
$HNO_{3,Morse}$	1.49×10^{-5}	5.57×10^{-7}	2.04×10^{-8}	1.39×10^{-9}	1.42×10^{-10}
HF_{DF}	1.82×10^{-5}	5.86×10^{-7}	1.86×10^{-8}	1.10×10^{-9}	9.32×10^{-11}
HCl_{DF}	6.41×10^{-6}	1.69×10^{-7}	2.00×10^{-9}	2.03×10^{-11}	7.88×10^{-14}
OH_{DF}	1.42×10^{-6}	2.46×10^{-7}	1.24×10^{-8}	9.22×10^{-10}	9.76×10^{-11}
$HCOOH_{DF}$	9.20×10^{-6}	5.72×10^{-7}	2.98×10^{-8}	2.57×10^{-9}	3.30×10^{-10}
CH_3OH_{DF}	3.08×10^{-6}	6.24×10^{-7}	3.30×10^{-8}	2.41×10^{-9}	2.77×10^{-10}
$HNO_{3,DF}$	1.48×10^{-5}	6.42×10^{-7}	3.19×10^{-8}	2.95×10^{-9}	3.98×10^{-10}

In Table 7, we present calculated Deng-Fan oscillator strengths for the OH-stretch in HNO_3, with the semi-empirical approach, using dipole moment functions calculated at various levels of theory.

Table 7: Calculated Deng-Fan oscillator strengths for the OH-stretch in HNO_3 with the semi-empirical approach. The dipole moment functions are calculated at various level of theory.

Δv	HF[a,b]	B3LYP[a,b]	B3LYP[a,b]	QCISD[a,b]	CCSD(T)[a,d]
1	3.09×10^{-5}	1.69×10^{-5}	1.60×10^{-5}	1.72×10^{-5}	1.48×10^{-5}
2	5.81×10^{-7}	7.01×10^{-7}	6.29×10^{-7}	7.11×10^{-7}	6.42×10^{-7}
3	3.35×10^{-8}	4.47×10^{-8}	4.02×10^{-8}	3.61×10^{-8}	3.19×10^{-8}
4	3.20×10^{-9}	4.04×10^{-9}	3.95×10^{-9}	3.24×10^{-9}	2.95×10^{-9}
5	4.25×10^{-10}	4.92×10^{-10}	5.43×10^{-10}	4.20×10^{-10}	3.98×10^{-10}

[a] Taken from ref. [5].
[b] With the 6-311++G(2d,2p) basis set.
[c] With the 6-311++G(3df,3pd) basis set.
[d] With the aug-cc-pVTZ basis set.

As seen in Table 7, the calculated oscillator strengths are somewhat sensitive to the level of theory used to calculated the dipole moment function.

7 HCl Overtone Intensities

To illustrate the discrepancy observed for the oscillator strengths for v=4 and v=5 for HCl, we separate the contributions to the oscillator strengths in the following way:

$$|\underbrace{\langle 0|\vec{\mu}|v\rangle}_{C}| = |\langle 0|\underbrace{\mu_1 q}_{A'} + \underbrace{\mu_2 q^2 + \mu_3 q^3 + \mu_4 q^4 + \mu_5 q^5 + \mu_6 q^6}_{B'}|v\rangle|. \tag{7.1}$$

We now define the following terms

$$A = \langle 0|A'|v\rangle \quad \& \quad B = \langle 0|B'|v\rangle. \tag{7.2}$$

The dipole moment coefficients for HCl calculated at the CCSD(T)/aug-cc-pV(T+d)Z level of theory are:

Molecule	μ_1[D/Å]	μ_2[D/Å^2]	μ_3[D/Å^3]	μ_4[D/Å^4]	μ_5[D/Å^5]	μ_6[D/Å^6]
HCl	0.9157	-0.0208	-0.6903	-0.2723	0.0917	0.2455

The displacement matrix elements for Δv=4 and Δv=5 for the Deng-Fan oscillator are:

Deng-Fan	$\langle 0\|q\|v\rangle$[Å]	$\langle 0\|q^2\|v\rangle$[Å^2]	$\langle 0\|q^3\|v\rangle$[Å^3]	$\langle 0\|q^4\|v\rangle$[Å^4]	$\langle 0\|q^5\|v\rangle$[Å^5]	$\langle 0\|q^6\|v\rangle$[Å^6]
$\Delta v = 4$	0.00033327	-0.00054493	0.00039225	-0.00008690	-0.00001284	-0.00001477
$\Delta v = 5$	-0.00009638	0.00017202	-0.00015614	0.00007049	-0.00000809	0.00000048

The displacement matrix elements for v=4 and v=5 for the Morse oscillator are:

Morse	$\langle 0\|q\|v\rangle$[Å]	$\langle 0\|q^2\|v\rangle$[Å^2]	$\langle 0\|q^3\|v\rangle$[Å^3]	$\langle 0\|q^4\|v\rangle$[Å^4]	$\langle 0\|q^5\|v\rangle$[Å^5]	$\langle 0\|q^6\|v\rangle$[Å^6]
$\Delta v = 4$	-0.00024075	0.00047355	-0.00038541	0.00009566	0.00001268	0.00001506
$\Delta v = 5$	-0.00005997	0.00013392	-0.00014194	0.00007214	-0.00000967	0.00000044

Combining these gives the following values of A, B and C:

Potential	A[D]	B[D]	C[D]	C^2[D^2]
v=4				
Deng-Fan	3.05175×10^{-4}	-2.4058×10^{-4}	6.45991×10^{-5}	4.17305×10^{-9}
Morse	-2.20455×10^{-4}	2.3501×10^{-4}	1.45557×10^{-5}	2.11868×10^{-10}
v=5				
Deng-Fan	-8.82552×10^{-5}	8.4387×10^{-5}	-3.86818×10^{-6}	1.49628×10^{-11}
Morse	-5.49145×10^{-5}	7.47732×10^{-5}	1.98587×10^{-5}	3.94367×10^{-10}

As seen from the last Table, the values of A differ by ∼28 % and ∼38 % for $\Delta v = 4$ and $\Delta v = 5$, respectively, whereas the values of B differ by ∼2 % and ∼11 % for $\Delta v = 4$ and $\Delta v = 5$, respectively. We can thereby conclude that the difference in oscillator strengths between the Morse and Deng-Fan oscillator for HCl (for Δv=4,5) originates predominately from the linear dipole contribution. For the Deng-Fan oscillator (of HCl for Δv=4 and 5), the linear contribution to the oscillator strength (A) is larger than the sum of higher order contributions (B), whereas the opposite is true for the Morse oscillator.

In figure 1, we present the calculated oscillator strengths for HCl using a linear and a non-linear dipole moment function.

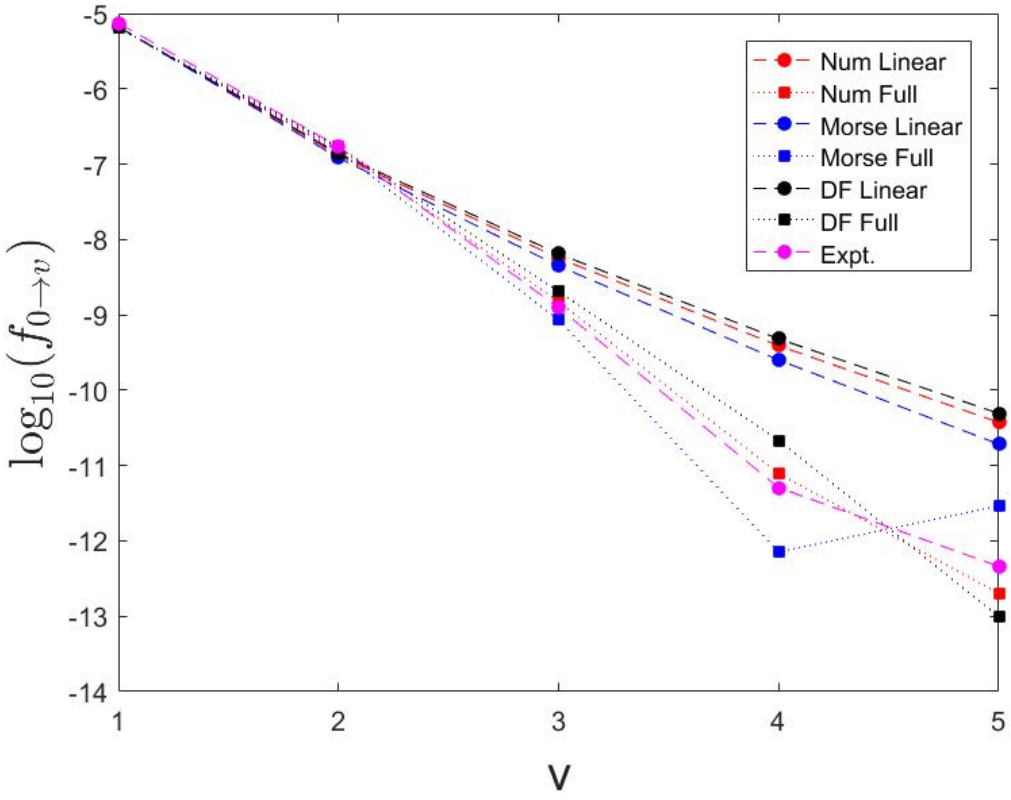

Figure 1: Calculated oscillator strengths for HCl with a linear and with a non-linear dipole moment function.

As seen from figure 1, a linear dipole moment function is not sufficient to get accurate oscillator strengths for HCl. The abnormally seen for v=4 and 5, for the Morse potential is due to cancelling terms in the transition dipole moment, as outlined in the previous section.

8 T_1-diagnostic

We have evaluated the T_1-diagnostics for a range of XH-stretching displacements (-0.3 Å to 0.6 Å) for all molecules. This range is greater than the classical turning point even for the calculated $v = 6$ wave functions for all XH-stretches considered. Singly excited determinants allow the molecular orbitals to relax in order to describe multi-reference character. As a consequence, the magnitude of the singles amplitude ($|\vec{t}_1|$) is an indication of how appropriate the Hartree-Fock wave function is as a reference state. The T_1-diagnostic is defined as

$$T_1 = \frac{1}{\sqrt{N_{elec}}}|\vec{t}_1| \tag{8.1}$$

For $T_1 < 0.02$, the multi-reference is believed to be minimal, and the CCSD(T) method will likely yield an accurate result [25].

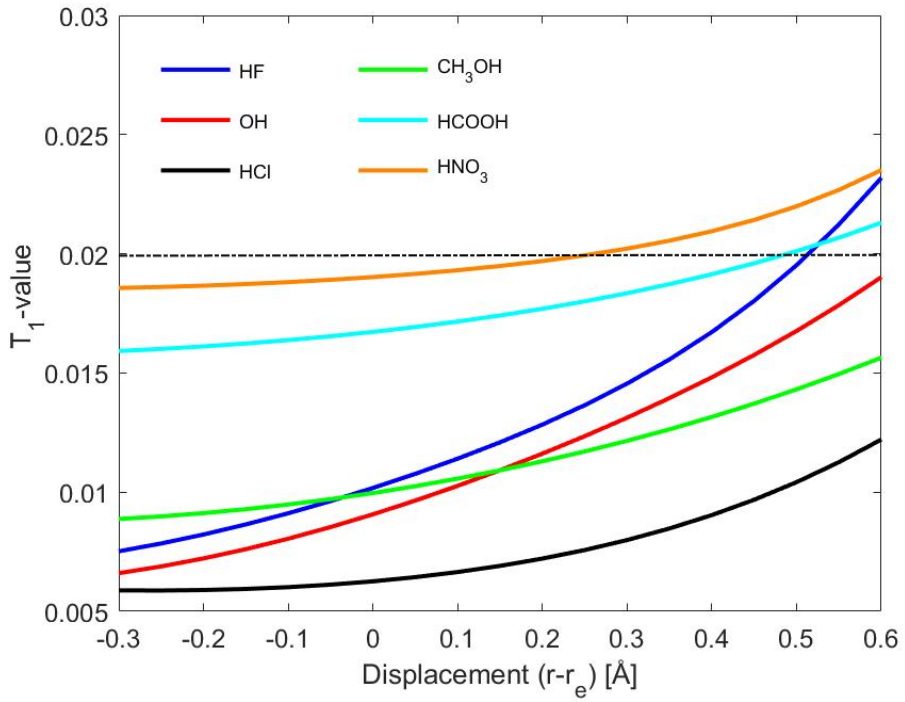

Figure 2: T_1-diagnostic along the XH-stretching displacement coordinate for hydrogen fluoride (blue), the hydroxyl radical (red), hydrogen chloride (black), methanol (green), formic acid (turquoise) and nitric acid (orange): The T_1-diagnostic is calculated for equally spaced (0.05 Å) points in the displacement range of -0.3 Å and 0.6 Å.

The classical turning points for the $v = 6$ wave functions of the numeric potentials are shown in Table 8.

Table 8: Classical turning points for the $v = 6$ wave functions for the numeric potentials in Å

Turning point	HF	OH	HCl	CH_3OH	HCOOH	HNO_3
Inner wall	-0.20	-0.22	-0.25	-0.21	-0.21	-0.22
Outer wall	0.40	0.45	0.50	0.45	0.45	0.45

It is evident from Table 8 and Figure 2, that based on the T_1-diagnostic, multi-reference character is only a potential problem for the higher overtones of the OH-stretch in nitric acid.

9 Molecular Geometries

Optimized molecular geometries of all molecules:

Table 9: Molecular geometries for the diatomic molecules optimized at the CCSD(T)/aug-cc-pVTZ (aug-cc-pV(T+d)Z for HCl) level of theory in MOLPRO

r_{FH} [Å]	r_{OH} [Å]	r_{HCl} [Å]
0.92099106	0.97325837	1.27637516

Table 10: Molecular geometry for CH_3OH optimized at the CCSD(T)/aug-cc-pVTZ level of theory in MOLPRO

CH_3OH						
C						
O	1	B1				
H	2	B2	1	A1		
H	1	B3	2	A2	3	180
H	1	B4	2	A3	3	D2
H	1	B4	2	A3	3	-D2

B1=1.42579143 Å, B2=0.96110307 Å, B3=1.08941466 Å, B4=1.09480995 Å
A1=107.99645707 °, A2=106.66319994 °, A3=111.84066932 °
D2=61.39542691 °

Table 11: Molecular geometry for HCOOH and HNO_3 optimized at the CCSD(T)/aug-cc-pVTZ level of theory in MOLPRO

HCOOH							HNO_3						
C							N						
O	1	B1					O	1	B1				
O	2	B2	1	A1			O	1	B2	2	A1		
H	1	B3	2	A2	3	180.0	O	1	B3	2	A2	3	180.0
H	1	B4	2	A3	3	0.0	H	4	B4	1	A3	3	0.0

HCOOH

B1=1.20395243 Å, B2=1.34801441 Å, B3=1.09470490 Å, B4=0.97007479 Å
A1=124.98826965 °, A2=125.12916605 °, A3=106.59838252 °

HNO_3

B1=1.19830239 Å, B2=1.21373216 Å, B3=1.40697773 Å, B4=0.97227516 Å
A1=130.40114999 °, A2=113.97719842 °, A3=102.03409186 °

References

[1] Z. H. Deng and Y. P. Fan, "A potential function of diatomic molecules," *Shandong University Journal*, vol. 7, pp. 162–166, 1957.

[2] A. D. S. Mesa, C. Quesne, and Y. F. Smirnov, "Generalized Morse potential: Symmetry and satellite potentials," *Journal of Physics A: Mathematical and General*, vol. 31, no. 1, pp. 321–335, 1998.

[3] M. Abramowitz and I. A. Stegun, "Handbook of mathematical functions: With formulas, graphs, and mathematical tables," *Courier Corporation*, vol. 55, 1964.

[4] Z. Rong and M. L. Sage, "Displacement matrix elements of Deng-Fan oscillators," *Interdisciplinary Sciences: Computational Life Sciences*, vol. 1, no. 3, pp. 163–167, 2009.

[5] Z. Rong, H. G. Kjaergaard, and M. L. Sage, "Comparison of the Morse and Deng-Fan potentials for XH bonds in small molecules," *Molecular Physics*, vol. 101, no. 14, pp. 2285–2294, 2003.

[6] D. U. Webb and K. N. Rao, "Vibration rotation bands of heated hydrogen halides," *Journal of Molecular Spectroscopy*, vol. 28, no. 2, pp. 121–124, 1968.

[7] L. Rothman, I. Gordon, A. Barbe, D. Benner, P. Bernath, M. Birk, V. Boudon, L. Brown, A. Campargue, J.-P. Champion, K. Chance, L. Coudert, V. Dana, V. Devi, S. Fally, J.-M. Flaud, R. Gamache, A. Goldman, D. Jacquemart, I. Kleiner, N. Lacome, W. Lafferty, J.-Y. Mandin, S. Massie, S. Mikhailenko, C. Miller, N. Moazzen-Ahmadi, O. Naumenko, A. Nikitin, J. Orphal, V. Perevalov, A. Perrin, A. Predoi-Cross, C. Rinsland, M. Rotger, M. Šimečková, M. Smith, K. Sung, S. Tashkun, J. Tennyson, R. Toth, A. Vandaele, and J. V. Auwera, "The {HITRAN} 2008 molecular spectroscopic database," *Journal of Quantitative Spectroscopy and Radiative Transfer*, vol. 110, no. 9–10, pp. 533 – 572, 2009. {HITRAN}.

[8] D. Rank, B. Rao, and T. Wiggins, "Molecular constants of HCl^{35}," *Journal of Molecular Spectroscopy*, vol. 17, no. 1, pp. 122–130, 1965.

[9] G. A. West, J. J. Barrett, D. R. Siebert, and K. V. Reddy, "Photoacoustic spectroscopy," *Review of Scientific Instruments*, vol. 54, no. 7, pp. 797–817, 1983.

[10] A. Sinha, R. L. Vander Wal, and F. F. Crim, "State-resolved unimolecular reactions: The vibrational overtone initiated decomposition of nitric acid," *The Journal of Chemical Physics*, vol. 92, no. 1, pp. 401–410, 1990.

[11] D. Hurtmans, F. Herregodts, M. Herman, J. Liévin, A. Campargue, A. Garnache, and A. Kachanov, "Spectroscopic and ab initio investigation of the ν_{OH} overtone excitation in trans-formic acid," *The Journal of Chemical Physics*, vol. 113, no. 4, pp. 1535–1545, 2000.

[12] D. L. Howard and H. G. Kjaergaard, "Resonance coupling in the fourth OH-stretching overtone spectrum of formic acid," *The Journal of Chemical Physics*, vol. 121, no. 1, pp. 136–140, 2004.

[13] M. Freytes, D. Hurtmans, S. Kassi, J. Liévin, J. Vander Auwera, A. Campargue, and M. Herman, "Overtone spectroscopy of formic acid," *Chemical Physics*, vol. 283, no. 1, pp. 47–61, 2002.

[14] D. Rueda, O. V. Boyarkin, T. R. Rizzo, A. Chirokolava, and D. S. Perry, "Vibrational overtone spectroscopy of jet-cooled methanol from 5000 to 14000 cm^{-1}," *The Journal of Chemical Physics*, vol. 122, no. 4, 044314. 2005.

[15] O. Boyarkin, L. Lubich, R. Settle, D. Perry, and T. Rizzo, "Intramolecular energy transfer in highly vibrationally excited methanol. I. Ultrafast dynamics," *The Journal of Chemical Physics*, vol. 107, no. 20, pp. 8409–8422, 1997.

[16] K. Feierabend, D. Havey, and V. Vaida, "Gas phase spectroscopy of HNO_3 in the region 2000–8500cm^{-1}," *Spectrochimica Acta Part A: Molecular and Biomolecular Spectroscopy*, vol. 60, no. 12, pp. 2775–2781, 2004.

[17] D. Donaldson, J. Orlando, S. Amann, G. Tyndall, R. Proos, B. Henry, and V. Vaida, "Absolute intensities of nitric acid overtones," *The Journal of Physical Chemistry A*, vol. 102, no. 27, pp. 5171–5174, 1998.

[18] S. S. Brown, R. W. Wilson, and A. Ravishankara, "Absolute intensities for third and fourth overtone absorptions in HNO_3 and H_2O_2 measured by cavity ring down spectroscopy," *The Journal of Physical Chemistry A*, vol. 104, no. 21, pp. 4976–4983, 2000.

[19] B. J. Miller, L. Du, T. J. Steel, A. J. Paul, A. H. Sodergren, J. R. Lane, B. R. Henry, and H. G. Kjaergaard, "Absolute intensities of NH-stretching transitions in dimethylamine and pyrrole," *The Journal of Physical Chemistry A*, vol. 116, no. 1, pp. 290–296, 2011.

[20] K. M. Ervin and V. F. DeTuri, "Anchoring the gas-phase acidity scale," *The Journal of Physical Chemistry A*, vol. 106, no. 42, pp. 9947–9956, 2002.

[21] J. Berkowitz, G. B. Ellison, and D. Gutman, "Three methods to measure RH bond energies," *The Journal of Physical Chemistry*, vol. 98, no. 11, pp. 2744–2765, 1994.

[22] B. Ruscic, D. Feller, D. A. Dixon, K. A. Peterson, L. B. Harding, R. L. Asher, and A. F. Wagner, "Evidence for a lower enthalpy of formation of hydroxyl radical and a lower gas-phase bond dissociation energy of water," *The Journal of Physical Chemistry A*, vol. 105, no. 1, pp. 1–4, 2001.

[23] S. J. Blanksby and G. B. Ellison, "Bond dissociation energies of organic molecules," *Accounts of chemical research*, vol. 36, no. 4, pp. 255–263, 2003.

[24] Y. Luo, "Handbook of bond dissociation energies in organic molecules," *CRC Press, Boca Raton*, 2003.

[25] T. J. Lee and P. R. Taylor, "A diagnostic for determining the quality of single-reference electron correlation methods," *International Journal of Quantum Chemistry*, vol. 36, no. S23, pp. 199–207, 1989.